Indian Journal of Pure & Applied Physics
Vol. 57, September 2019, pp. 619-623

Incomplete momentum transfer in ^{16}O + ^{148}Nd system [at energy ≈ 5.8 MeV/nucleon]

Pankaj K Giri[a], Amritraj Mahato[a], D Singh[a*], Sneha B Linda[a], Harish Kumar[b], Suhail A Tali[b], R Ali[c], N P M Sathik[d], M Afzal Ansari[b], R Kumar[e], S Muralithar[e] & R P Singh[e]

[a]Department of Physics, Central University of Jharkhand, Ranchi 835 205, India

[b]Department of Physics, Aligarh Muslim University, Aligarh 202 002, India

[c]Department of Physics, G F (P G) College, Shahjahanpur 242 001, India

[d]Department of Physics, Jamal Mohammed College, Tiruchirappalli 620 020, India

[e]Inter University Accelerator Centre, Aruna Asaf Ali Marg, New Delhi 110 067, India

Received 3 July 2019

Measurements of the forward recoil ranges of the evaporation residues ^{159,158}Er (xn), ^{160g,159}Ho (pxn), ^{157,155}Dy (αxn) and ^{155}Tb (αpxn) formed in the interaction of ^{16}O with ^{148}Nd at energy ≈ 5.8 MeV/nucleon have been done. Measured forward recoil range distributions of these evaporation residues show population of several incomplete fusion channels in addition to complete fusion. The entire and incomplete linear momentum transfers inferred from these recoil range distributions have been used to identify the evaporation residues populated through complete and incomplete fusion dynamics. The forward recoil range distributions of evaporation residues populated via α-emission channels show two composite peaks, one associated with complete fusion and other peak corresponds to the incomplete fusion. Further, the relative contributions of CF and/or ICF components have also been separated out from the present measurements. The contribution of ICF channels has been found to be ≈ 9 % of total fusion. The present results clearly indicate the presence of break-up of the projectile ^{16}O into ^{12}C + α at low projectile energy.

Keywords: Complete and incomplete fusion, Composite system, Offline γ -ray spectrometry, Recoil catcher activation technique, Recoil range distributions

1 Introduction

The dominant modes of heavy ion interactions are compound nucleus (CN) and direct reactions at projectile energies close to Coulomb barrier. The probability of formation of compound nucleus gets hindered with increasing the projectile energy and incomplete fusion (ICF) starts dominating with complete fusion (CF). In ICF reactions, only a part of the projectile fuses with the target while the remaining part moves at forward angles with approximately same velocity of projectile. A schematic diagram of CF and ICF reactions is shown in Fig. 1. These reactions were first observed experimentally by Britt and Quinton[1] and Galin *et al*.[2]. Later on, remarkable studies based on particle-gamma coincidence technique by Inamura *et al*.[3] contributed a lot to understand the dynamics of ICF reactions. Various dynamical models have been proposed to explain the mechanism of ICF reactions. In the sum rule model of Wilczynski *et al*.[4], ICF is considered as arising from peripheral collisions in the angular momenta range just above the critical angular momentum $\left(\ell_{crit}\right)$ for CF. Udagawa & Tamura[5] explained ICF as breakup of the projectile followed by fusion of one of the fragments with the target. The promptly emitted particle (PEP) model[6], hot spot model[7], multistep direct reaction model[8], etc., are also some of the widely used theoretical models. All these models have been used to reproduce the experimental data at energy above 10 MeV/nucleon. There are many important aspects of ICF reactions at low projectile energy that should be clarified such as, how the ICF dynamics depends on various entrance channel parameters and the angular momenta involved in these reactions. Morgenstern *et al*.[9] have reported that ICF is more dominant for more mass asymmetric system at same relative velocity. Several investigators have made efforts to understand the role

*Corresponding author (E-mail: dsinghcuj@gmail.com)

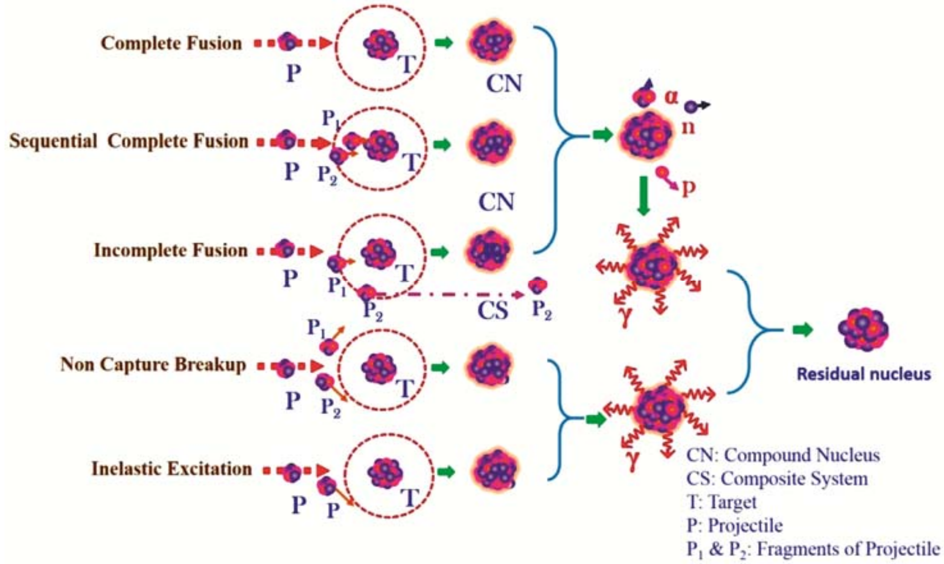

Fig. 1 – A pictorial representation of CF and ICF dynamics in heavy ion interaction.

of different entrance channel parameters on ICF dynamics[10-12]. Studies show that the ICF dynamics also depends on Coulomb factor[13] (Z_PZ_T) and deformation of target[14,15] (β_2^T). However, no definite conclusion has been established yet regarding the dependence of ICF on various entrance channel parameters.

The forward recoil range measurement provides significant information about the degree of linear momentum transfer in heavy ion interaction[16]. These measurements are useful to understand the mechanism of ICF reactions. In this paper, the results of forward recoil range distributions (FRRDs) of various evaporation residues populated through CF and ICF dynamics in the system ^{16}O + ^{148}Nd at beam energy ≈ 5.8 MeV/nucleon are presented. The CF and ICF contribution has also been deduced from the present FRRDs measurements in the studied energy.

2 Experimental Details

The experiment was performed at the 15 UD Pelletron accelerator at Inter University Accelerator Centre (IUAC), New Delhi, India. Thin target of metallic ^{148}Nd of thickness around 450 μg/cm^2 were prepared by vacuum evaporation technique by depositing on thin aluminum foils of thickness ≈1 mg/cm^2. A stack of 19 aluminum catcher foils having thickness of around 40-100 μg/cm^2, prepared by the same technique was used to stop the recoiling residues. The thickness of the targets and aluminum foils were measured by α-transmission method. The stopping power and range calculation software[17], SRIM-2008 was used to determine the energy loss of incident particles. In the stack, the target was mounted with the aluminum backing facing the beam. The target was bombarded with the ^{16}O projectile for ≈12 h at General purpose scattering chamber (GPSC) facility of IUAC, New Delhi. This chamber has an In-vacuum transfer facility (IVTF) and useful to reduce the time lapse between stop of irradiation and start of counting of samples. The beam current was ≈2 pnA, which was measured with a Faraday cup placed behind the target catcher assembly. After the irradiation, the activities of individual evaporation residues (ERs) were measured by high purity germanium detector (HPGe) connected to a PC through CAMAC based data acquisition system. The software CANDLE[18] was used for the online data recording and offline analysis of the measured data. The energy and efficiency calibration of the HPGe detector was done using the standard ^{152}Eu^g γ-ray source of known strength. The ERs have been identified by observing their characteristic γ-rays and also from their decay curve analysis. A typical γ-ray spectrum of induced activity in the Al-catcher foil corresponding to cumulative thickness ≈435 μg/cm^2 after the interaction of projectile ^{16}O with ^{148}Nd at energy ≈5.8 MeV/nucleon is displayed in Fig. 2. The yields for a particular ER in different catcher foils were obtained using the standard expression[19]:

$$\sigma_{ER}(E) = \frac{A\lambda \exp(\lambda t_2)}{N_0 \phi(\varepsilon_G).\theta.K[1-\exp(-\lambda t_1)][1-\exp(-\lambda t_3)]} \quad \cdot \quad \ldots(1)$$

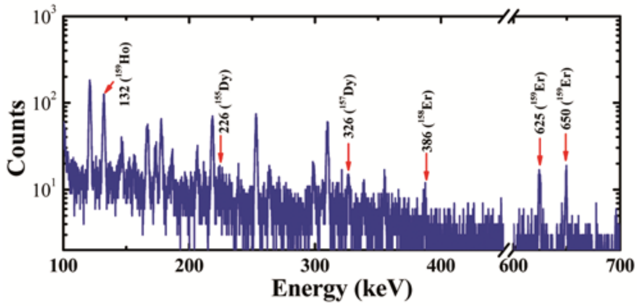

Fig. 2 – Typical γ-ray spectrum of induced activity in the Al-catcher foil corresponding to cumulative thickness ≈ 435 μg/cm^2 after the interaction of projectile ^{16}O with ^{148}Nd at energy ≈5.8 MeV/nucleon.

Where, A is the counts recorded for the characteristic γ-ray, λ is decay constant of the ER, N_0 is number of target nuclei per unit area, ϕ is the incident ion beam flux, ε_G is the geometry dependent efficiency, θ is the branching ratio of the characteristic γ-ray, t_1 is the irradiation time, t_2 is the time elapsed between stop of irradiation and start of the counting of the individual target along with backing and t_3 is the counting time. $K = \exp(-\mu d)$ is the correction for self-absorption of the gamma-ray with the absorption coefficient μ for the target of thickness 'd'. Several factors are responsible for the errors and uncertainties in the measured cross-sections. The main factors are: (i) the uncertainty due to the non-uniformity of the ^{148}Nd target, (ii) the uncertainty in the efficiency calibration of the 100 cc HPGe detector, (iii) the error arising from the fluctuations in current of the beam and (iv) uncertainty due to the straggling effect of the beam passing through the target catcher assembly. The overall uncertainty from several factors discussed above was estimated to be less than 15%.

3 Results and Discussion

Forward recoil range distributions (FRRDs) of the evaporation residues $^{159,158}Er(xn)$, $^{160g,159}Ho(pxn)$, $^{157,155}Dy(\alpha xn)$ and $^{155}Tb(\alpha pxn)$ produced via complete and/or incomplete fusion have been measured in the ^{16}O + ^{148}Nd system at projectile energy ≈5.8 MeV/nucleon. The measured yield of the ERs in each catcher foil has been divided by its thickness to obtain the normalized yield of a particular ER. These normalized yields of the different ERs have been plotted as function of cumulative catcher thickness to obtain differential recoil range distributions of the identified ERs. The relative contributions of various

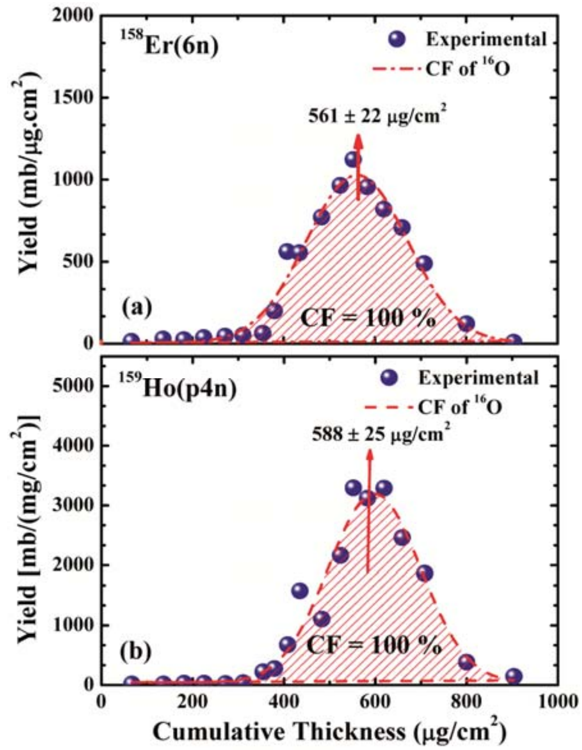

Fig. 3 – Measured FRRDs for the ERs $^{159}Er(5n)$ and $^{159}Ho(p4n)$ produced in ^{16}O + ^{148}Nd system at energy ≈5.8 MeV/nucleon. Solid circles represent the measured data and dashed dotted curves represent the Gaussian fit to the measured FRRDs.

ERs produced via CF and/or ICF processes have been computed by fitting the measured FRRDs data with Gaussian composite peaks using the ORIGIN software[20]. The more details about the analysis of FRRDs are given in our earlier work[16]. The theoretical forward recoil ranges of ERs have been computed using code[17] SRIM-2008. The measured forward recoil range distributions (FRRDs) of identified ERs have been compared with the theoretical mean ranges. As a representative case, FRRDs of ERs $^{158}Er(6n)$, $^{159}Ho(p4n)$, $^{157}Dy(\alpha 3n)$, and $^{155}Dy(\alpha 5n)$ have been displayed in Figs 3 and 4. It can be clearly observed from Fig. 3 that measured forward recoil range distributions (FRRDs) of ERs $^{158}Er(6n)$ and $^{159}Ho(p4n)$ shows only single peak corresponding to cumulative thickness ≈ 561 and ≈588 μg/cm^2 , respectively. The theoretically estimated mean recoil range corresponding to CF of ^{16}O projectile is ≈583 μg/cm^2 calculated using SRIM-2008 code. The measured most probable ranges and theoretically estimated mean ranges have been found to be in good agreement. This agreement reveals that the ERs $^{158}Er(6n)$ and $^{159}Ho(p4n)$ are populated through CF of projectile ^{16}O with ^{148}Nd target. On the other hand, the

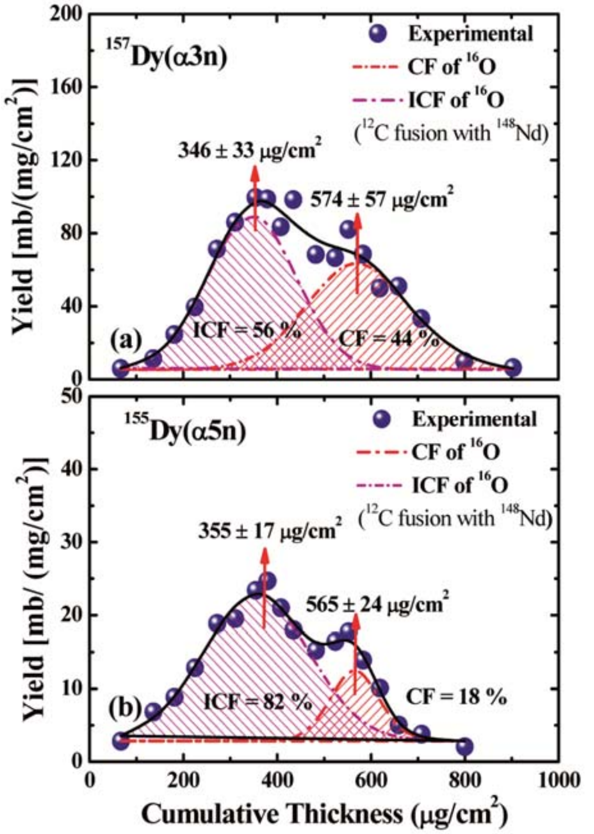

Fig. 4 – Measured FRRDs for the ERs ^{157}Dy(α3n) and ^{155}Dy(α5n) produced in ^{16}O + ^{148}Nd system at energy ≈5.8 MeV/nucleon. Solid circles represent the measured data and dashed dotted curves represent the Gaussian fit to the measured FRRDs.

observed FRRDs for the evaporation residue ^{157}Dy populated through α3n channel shows two Gaussian peaks corresponding to mean cumulative thickness ≈346 and ≈574 μg/cm^2 as shown in Fig. 4(a). Similarly, the ER ^{155}Dy(α5n) also shows two peaks corresponding to mean cumulative thickness ≈355 and ≈565 μg/cm^2 as shown in Fig. 4(b). The peak corresponding to larger cumulative catcher thickness can be referred to CF of ^{16}O, while the other peak at shorter cumulative thickness is associated with ICF of ^{16}O, (i.e., fusion of fragment ^{12}C). These FRRDs results shows that full and incomplete linear momentum transfer components are involved and the ERs are populated through both CF and ICF dynamics. Further, to separate out the relative contributions of ERs populated via CF and ICF channels from measured FRRDs data in ^{16}O + ^{148}Nd system at projectile energy ≈ 5.8 MeV/nucleon, an attempt has been made. The areas under the composite peaks in FRRDs of ERs populated via CF and/or ICF dynamics have been computed. The relative

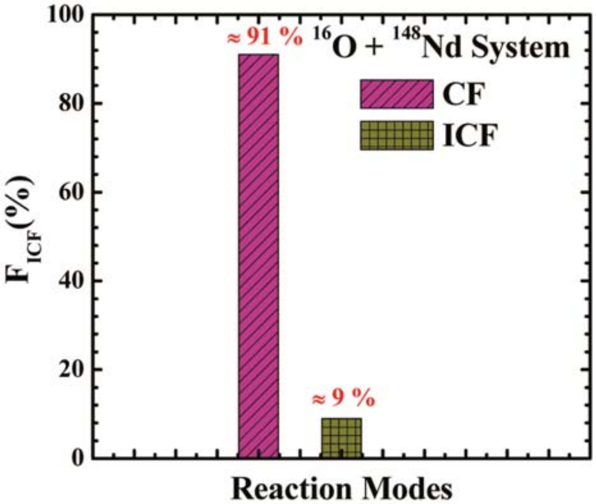

Fig. 5 – The relative contribution of CF and ICF channels in the measurement of FRRDs for the system ^{16}O + ^{148}Nd at energy ≈5.8 MeV/nucleon.

contributions of both the CF and ICF components are obtained by dividing the area of the corresponding peak by the total area under the observed composite FRRDs curve. The relative contribution of CF of ^{16}O with the target ^{148}Nd for the ERs ^{158}Er(6n) and ^{159}Ho(p4n) are found to be ~100% and shown in Fig. 3(a) and (b). However, for the ERs ^{157}Dy(α3n), and ^{155}Dy(α5n), the relative contributions of the ICF of the projectile ^{16}O by fusion of fragment ^{12}C with the target ^{148}Nd is found to be ~ 56% and ~ 82% , respectively as displayed in Fig. 4, while for same ERs, the CF contribution is found to be ~ 44% and 18%, respectively. The total contribution of complete and incomplete fusion channels has also been estimated and displayed in Fig. 5. The contribution of CF channels has been found to be ≈91 % of total fusion, while the ICF contribution has been observed ≈9 %. The present results clearly indicate the presence of break-up of the incident projectile ^{16}O into *α* clusters, (i.e., ^{12}C + *α*) at these low projectile energies.

4 Conclusions

In the present work, forward recoil range distributions (FRRDs) of evaporation residues ^{159,158}Er(xn), ^{160g,159}Ho(pxn), ^{157,155}Dy(αxn) and ^{155}Tb(αpxn) populated via CF and ICF dynamics in the system ^{16}O + ^{148}Nd at energy range ≈5.8 MeV/nucleon have been measured. The recoil range distributions have been fitted by Gaussian peaks using the software ORIGIN and compared with the theoretically calculated mean ranges from software SRIM-2008. The measured FRRDs of evaporation residues populated via xn/pxn channels show one peak, which indicate the production of these ERs through CF only. Two composite peaks have been observed in the measured FRRDs of ERs formed via α-emission channels. The present FRRDs results strongly reveal a significant contribution from the incomplete linear momentum transfer in the production of evaporation residues via α-emitting channels. Further, an attempt has also been made to separate out the relative contributions of CF and/or ICF components from the present measurements. The contribution of ICF channels has been found to be ≈ 9 % of total fusion. On the basis of present analysis, it may be concluded that incomplete fusion plays vital role in the production of various reaction products involving direct *α*-cluster emission at low projectile energy.

Acknowledgement

Authors are grateful to the Director and Convener AUC, IUAC, New Delhi for providing the necessary experimental facilities. Authors are thankful to the target lab in-charge, Mr Abhilash S R and operational staff of pelletron accelerator, IUAC for their support and help during the course of experiment. One of the authors DS express sincere thanks to the Vice - Chancellor, Central University of Jharkhand, Ranchi for encouragement during the entire work. Authors are also thankful to Head, Department of Physics, CUJ, Ranchi for their motivation and support throughout the work.

References

1 Britt H C & Quinton A R, *Phys Rev*, 124 (1994) 877.
2 Galin J, Catty B, Guerreau D, Rousset C, Schlotthauer-Voos U C & Tarrago X, *Phys Rev C*, 9 (1974) 1126.
3 Inamura T, Kojima T, Nomura T, Sugitate T & Utsunomiya H, *Phys Lett B,* 84 (1979) 71.
4 Wilczynski J, Siwek-Wilczynska K, van Driel J, Gonggrijp S, Hageman D C J M, Janssens R V F, Łukasiak J & Siemssen R H, *Phys Rev Lett*, 45 (1980) 606.
5 Udagawa T & Tamura T, *Phys Rev Lett*, 45 (1980) 1311.
6 Bondrof J P, De J N, Fai G, Karvinen A O T & Randrup J, *Nucl Phys A*, 333 (1980) 285.
7 Weiner R & Westrom M, *Nucl Phys A*, 286 (1977) 282.
8 Zegrebaev V & Penionzhkevich Y, *Prog Part Nucl Phys*, 35 (1995) 575.
9 Morgenstern H, Bohen W, Galster W, Grabisch K & Kyanowski A, *Phys Rev Lett*, 52 (1984) 1104.
10 Kumar H, Tali S A, Ansari M A, Singh D, Ali R, Kumar K, Sathik N P M, Ali A, Parashari S, Dubey R, Bala I, Kumar R, Singh R P & Muralithar S, *Eur Phys J A,* 54 (2018) 47.
11 Tali S A, Kumar H, Ansari M A, Ali A, Singh D, Giri P K, Linda S B, Parashari S, Kumar R, Singh R P & Muralithar S, *Nucl Phys A*, 970 (2018) 208.
12 Singh D, Giri P K, Mahato A, Linda S B, Kumar H, Ansari M A, Ali R, Tali S A, Rashid M H, Guin R & Das S K, *Nucl Phys A,* 981 (2019) 75.
13 Shuaib M, Sharma V R, Yadav A, Singh P P, Sharma M K, Singh D P, Kumar R, Singh R P, Muralithar S, Singh B P & Prasad R, *Phys Rev C,* 94 (2016) 014613.
14 Singh D, Linda S B, Giri P K, Mahato A, Tripathi R, Kumar H, Ansari M A, Sathik N P M, Ali R, Kumar R, Muralithar S & Singh R P, *Phys Lett B*, 774 (2017) 7.
15 Singh D, Linda S B, Giri P K, Mahato A, Tripathi R, Kumar H, Tali S A, Parashari S, Ali A, Dubey R, Ansari M A, Kumar R, Muralithar S & Singh R P, *Phys Rev C,* 97 (2018) 064610.
16 Singh D, Ali R, Ansari M A, Rashid M H, Guin R & Das S K, *Phys Rev C,* 79 (2009) 054601.
17 The Stopping and Range of Ions in Matter (SRIM-2008.04), URL: https://www.srim.org.
18 Kumar B P A, Subramaniam E T & Bhowmik R K, Con Proc DAE SNP (Kolkata, 2001); URL: http://www.iuac.res.in/NIAS/.
19 Ansari M A, Singh R K Y, Sehgel M L, Mittal V K, Avasthi D K & Govil I M, *Ann Nucl Energy,* 11 (1984) 607.
20 ORIGIN (Origin Lab, Northampton, MA); Web link “http://www.originlab.com/”.